Original Research Article

Achieving robust synthetic tolerance in industrial *E. coli* through negative auto-regulation of a DsrA-Hfq module

Xiaofeng Yang [a,*], Jingduan Yang [a], Haozheng Huang [a], Xiaofang Yan [a], Xiaofan Li [a], Zhanglin Lin [a,b,**]

[a] *School of Biology and Biological Engineering, South China University of Technology, Guangzhou, 510006, China*
[b] *School of Biomedicine, Guangdong University of Technology, Guangzhou 510006, China*

ABSTRACT

In industrial fermentation processes, microorganisms often encounter acid stress, which significantly impact their productivity. This study focused on the acid-resistant module composed of small RNA (sRNA) DsrA and the sRNA chaperone Hfq. Our previous study had shown that this module improved the cell growth of *Escherichia coli* MG1655 at low pH, but failed to obtain this desired phenotype in industrial strains. Here, we performed a quantitative analysis of DsrA-Hfq module to determine the optimal expression mode. We then assessed the potential of the CymR-based negative auto-regulation (NAR) circuit for industrial application, under different media, strains and pH levels. Growth assay at pH 4.5 revealed that NAR-05D04H circuit was the best acid-resistant circuit to improve the cell growth of *E. coli* MG1655. This circuit was robust and worked well in the industrial lysine-producing strain *E. coli* SCEcL3 at a starting pH of 6.8 and without pH control, resulting in a 250 % increase in lysine titer and comparable biomass in shaking flask fermentation compared to the parent strain. This study showed the practical application of NAR circuit in regulating DsrA-Hfq module, effectively and robustly improving the acid tolerance of industrial strains, which provides a new approach for breeding industrial strains with tolerance phenotype.

1. Introduction

During biomanufacturing, microbial cells often encounter various stresses, including the exposure to high levels of oxygen, high temperatures, and low pH values, which reduce the cell growth and productivity [1–4]. Acid stress is a major concern in industrial fermentation, as the accumulation of acidic products or byproducts occurs during cellular metabolism, particularly in the production of organic acids or amino acids [5,6]. The traditional strategy of adding base to maintain neutral pH in fermentation broth increases the utilization of neutralizing reagents, downstream process separation cost, and waste streams [7]. Therefore, the utilization of acid-tolerant strains for industrial fermentation is considered an effective route to achieving green bio-manufacturing [8–10].

Acid resistance (AR) in microorganisms is a complex trait that requires the cooperation of multiple genes and a sophisticated regulatory network [11]. Simply increasing the expression of a single functional gene is insufficient to achieve enough acid-tolerance characteristics in cells [12,13]. Thus, global regulation strategies that can regulate the expression profile of the entire gene network are commonly employed to develop stress-tolerance strains, including the common-used adaptive laboratory evolution (ALE) [14–16], and several alternative approaches like iterative CRISPR enabled trackable genome engineering (iCREATE) [17], and global transcription machinery engineering (gTME) [18–20].

One promising target for engineering microorganisms towards desired stress-tolerance phenotypes is RpoS, a global regulator that plays a crucial role in the general stress response in *E. coli* [13,21,22]. However, overexpressing RpoS alone does not effectively enhance the acid-tolerance of strains, likely due to its rigorous regulatory process [23,24]. Small noncoding RNAs (sRNAs), such as DsrA, RprA, and ArcZ, are involved in stabilizing and activating the translation of *rpoS* mRNA, at the post-transcriptional and translational levels [25,26].

Overexpressing these sRNAs, either individually or in combination, significantly improves the survival rate of *E. coli* under extreme-pH conditions (*e.g.* pH 2.5) [23], while their impact on growth performance is negligible under the moderate acid stress (*e.g.* pH 4.5) [27]. On the other hand, the RNA chaperone Hfq acts as an important mediator for sRNA-dependent gene expression by facilitating the annealing of these sRNAs to the *rpoS* 5′ untranscribed region (UTR) and protecting them from degradation [22,23,28]. In a previous study, we demonstrated that overexpressing DsrA along with Hfq significantly improved the acid-tolerance of cells in a lab strain MG1655, resulting in a 40–72% increase in biomass at pH 4.5 [27]. However, we further found that this DsrA-Hfq module impaired the cell growth when overexpressed in an industrial strain used for lysine production (Fig. S1).

Thus, we aimed to develop a reliable method for engineering industrial strains that exhibit the desired phenotypes observed in lab strains through the design of gene circuits [29,30]. Negative auto-regulation (NAR) circuits have shown great potential for this purpose due to their ability to reduce noise in gene expression [31], exhibit low growth-rate dependence [32], linearize dose responses [33], and mitigate growth burden caused by regulatory proteins [34]. In this study, we engineered a DsrA-Hfq module with a NAR circuit to develop a robust synthetic tolerance. We investigated the impact of the expression level of the DsrA-Hfq module on the acid-tolerance of *E. coli* and determined the optimal expression pattern for DsrA-Hfq. Meanwhile, we constructed a NAR circuit using a CymO operator, and evaluated the robustness of this circuit under difference media, pH levels and strains. We then adapted this NAR circuit to the DsrA-Hfq module to address the issue of DsrA-Hfq module losing its acid-tolerance performance in industrial lysine-producing strain *E. coli* SCEcL3. Without pH control in shake flasks, the best circuit resulted in the industrial strain exhibiting improved lysine titer compared with the parent strain. This study provides a useful approach for designing gene circuit to enhance the production robustness of industrial strains at low fermentation pH.

2. Materials and methods

2.1. Strains, plasmids, and materials

The strains and plasmids used in this study are listed in Table S1 and Table S2. *E. coli* DH10B, used for the plasmid construction, was cultured in Luria-Bertani (LB) with 34 μg/mL chloramphenicol. The DNA sequences of the primers used in this study are listed in Table S3.

Briefly, the *sfGFP*, *lacI, dsrA* and *hfq* genes and the pACYC184 backbone were amplified via polymerase chain reaction (PCR). The constitutive promoters, *lacO* and *cymO* operator were introduced through PCR amplification using oligo DNAs. The *cmyR* gene was synthetized by Generay Biotechnology (Shanghai, China). The plasmids for fluorescent characterization was constructed by assembling two DNA fragments, the *sfGFP* gene and pACYC184 backbone. For the constitutive acid-resistant plasmids, the *dsrA* and *hfq* cassettes along with constitutive promoters were assembled together using overlap PCR, and then the assembled DNA products were inserted into the pACYC184 backbone. To generate pCDTH or NAR circuit plasmids, similar procedures were applied. The deviation lies in the addition of LacO or CymO operator to the *dsrA* and *hfq* fragments by primers and PCR products of *lacI* and *cmyR*. All the plasmids in this study were constructed by Gibson Assembly [35].

Q5 DNA polymerase used for gene amplification, T5 exonuclease, Phusion High-Fidelity DNA polymerase and Taq DNA ligase used for Gibson assembly were purchased from New England Biolabs (Beverly, MA, USA). Oligonucleotides synthesis and sequence analysis were performed by Sangon Biotech (Shanghai, China). The kits for DNA purification, gel recovery, genomic DNA extraction and plasmid mini-prep were purchased from Tiangen (Beijing, China). The 96 well black flat clear bottom polystyrene microplates were purchased from Corning (New York, USA). All chemicals were purchased from Sigma-Aldrich

(Shanghai, China) or Sangon Biotech (Shanghai, China).

2.2. Fluorescence measurement

E. coli MG1655 or *E. coli* DH10B cells with corresponding plasmids (plasmids listed in Table S1) grown in LB medium with 34 μg/mL chloramphenicol. Overnight cultures were inoculated at a 1:50 vol/vol ratio in 196 μL LBG medium (LB medium supplemented with 2% glucose, pH 7.0/4.5) or M9 medium (pH 7.0/4.5) at 37 °C in a 96-well plate (Corning, USA). The fluorescence (ex/em 476/516 nm) and the optical density at 600 nm (OD$_{600}$) were measured using an Infinite® 200 PRO microplate reader (TECAN, Switzerland) for 6–8 h depending on the cell growth.

2.3. Cell growth assay

The cell growth assays were performed using a modification of the protocol as described in our previous study [27]. Wild-type *E. coli* MG1655 and strains harboring acid-resistant modules were cultured overnight (about 16 h) in LB medium (pH 7.0) at 37 °C. The cultures were then diluted to initial OD$_{600}$ 0.05 in 300 μL of LBG medium (pH 4.5) acidified with HCl. The cultures were incubated at 37 °C in 100-well Honeycomb microplates monitored by automated turbidimeter (Bioscreen C, Oy Growth Curves Ab Ltd., Helsinki, Finland) for online monitoring of OD$_{600}$ for 24 h. Each experiment was performed in three biological replicates.

2.4. Correlation analysis

Fluorescence data presented in Fig. S2 and Fig. S3A were logarithmically transformed using base 10 and considered as the corresponding expression levels of DsrA or Hfq. By integrating these data with the growth assay results shown in Fig. 1A, Fig. S3, we conducted a correlation analysis between the final OD$_{600}$ and the growth rate using IBM® SPSS® Statistics 22 software.

2.5. D value

The *D* value is defined as the ratio of fluorescence intensity in different environments using the following formula:

$$D_M = log_{10}(F_{M9} / F_{LBG}) \qquad \text{Eq. (1)}$$

$$D_S = log_{10}(F_{DH10B} / F_{MG1655}) \qquad \text{Eq. (2)}$$

$$D_{pH} = log_{10}(F_{7.0} / F_{4.5}) \qquad \text{Eq. (3)}$$

D_M represents the difference coefficient in different media, F_{M9} represents the fluorescence intensity in M9 medium, and F_{LBG} represents the fluorescence intensity in LBG medium. D_S represents the difference coefficient in different strains, F_{DH10B} represents the fluorescence intensity in DH10B strain, and F_{MG1655} represents the fluorescence intensity in MG1655 strain. D_{pH} represents the difference coefficient at pH, $F_{7.0}$ represents the fluorescence intensity at pH 7.0, and $F_{4.5}$ represents the fluorescence intensity at pH 4.5.

2.6. Fermentation in shake flasks

The seed medium and fermentation medium were prepared according to the formulation described in our previously published study [36]. Briefly, the seed medium consisted of sucrose (3 g/L), yeast extract (5 g/L), tryptone (7 g/L), ammonium sulfate (5 g/L), potassium dihydrogen phosphate (5 g/L), magnesium sulfate (0.5 g/L), ferrous sulfate (0.012 g/L), manganous sulfate (0.012 g/L), sodium glutamate (5 g/L), ʟ-threonine (0.3 g/L), ʟ-methionine (0.3 g/L) and pyruvic acid (0.3 g/L), and the fermentation medium consisted of glucose (30 g/L), phosphoric acid (0.6 g/L), magnesium sulfate (2 g/L), ammonium sulfate (10 g/L),
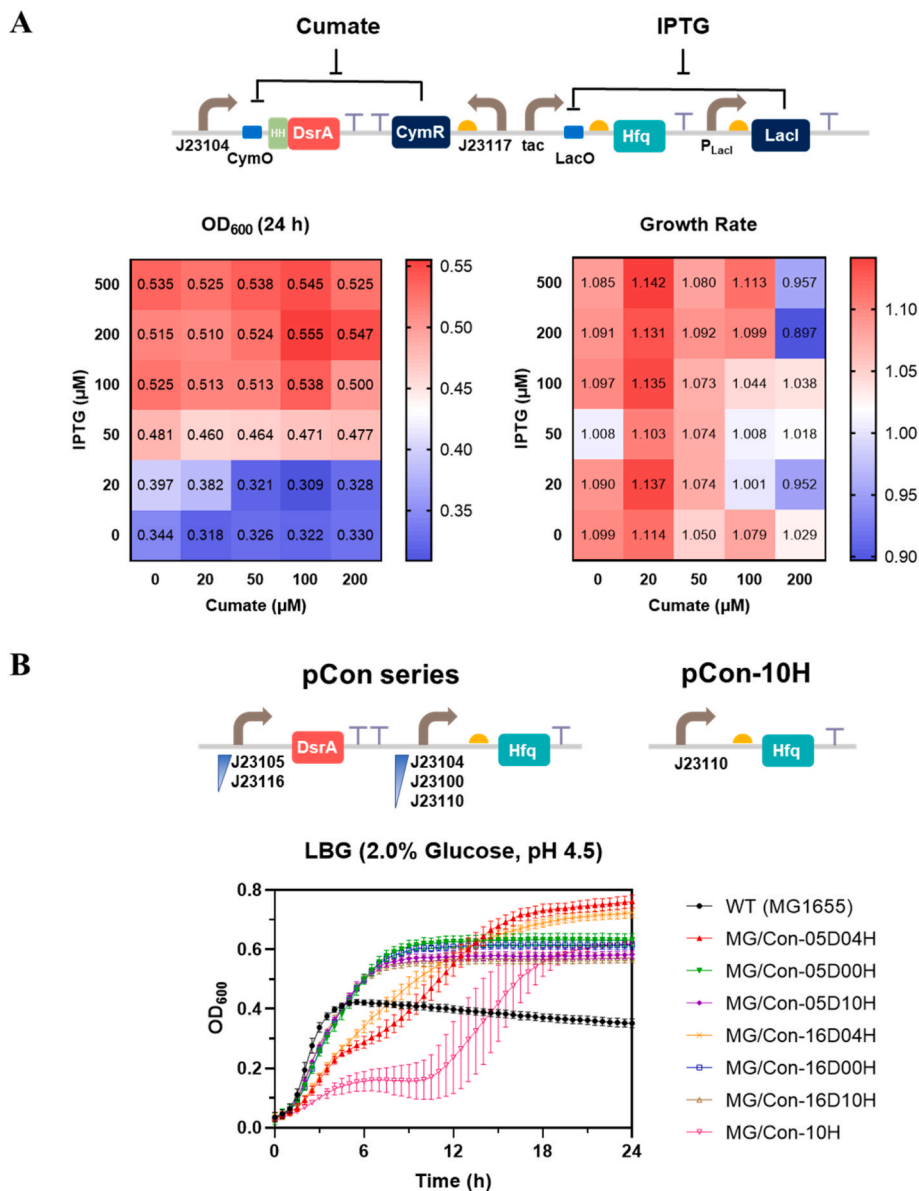
Fig. 1. Effect of DsrA and Hfq on the growth of *E. coli* in acidic condition. (A) Schematic representation of plasmid pCDTH. The P_{cymR} consisted of the J23104 promoter and the cymO operator, while the P_{tac} was composed of the tac promoter and the LacO operator. Final OD_{600} and growth rate of the strain harbored plasmid pCDTH with varying concentration of IPTG and cumate in LBG medium (pH 4.5) were presented under the schematic. (B) Schematic representation of pCon series plasmids and plasmid pCon-10H. Growth curve of strains with different pCon series plasmids in LBG medium (pH 4.5) were presented under the schematics.

corn steep liquor (0.325 g/L), potassium chloride (0.5 g/L), betaine (2.2 g/L), ferrous sulfate (0.032 g/L), manganous sulfate (0.032 g/L), L-threonine (0.25 g/L), cupric sulfate (6.8 mg/L), zinc sulfate (7.65 mg/L), and thiamine (5.6 mg/L). For the strains harboring plasmids with chloramphenicol resistance, 34 µg/mL chloramphenicol was added to the medium. Cells were activated in seed medium at 37 °C, 220 rpm until the OD_{600} reaching approximately 2.0. Seed cultures were inoculated at a ratio of 15 % (v/v) into 50 mL flasks containing 15 mL of fermentation medium, serving as the working volume. Fermentations were conducted at a starting pH of 6.8 and without pH control for 48 h cultivation. This time point was considered as the initial time point. Culture the cells at 37 °C, 220 rpm for 48 h. At 0 h, 3 h, 6 h, 12 h, 24 h, 36 h, and 48 h, 200 µL of each sample was transferred to 1.5 mL Eppendorf tubes. Measure pH by SevenCompact S210 pH meter (Mettler Toledo, Greifensee, Swiss) and OD_{600} by ultraviolet spectrophotometer (UV755B, Yoke Instrument, Shanghai, China). Centrifuge the samples at 4000 rpm, dilute the supernatant at 1:100 ratio for residual glucose

and lysine titer measurement using SBA-40D biosensor analyzer (Shandong Academy of Science, Shandong Province, China).

2.7. Evaluation of the lysine producing strains harboring auto-negative regulatory acid-resistant circuit by 2-mL micro-bioreactor (BioLector) fermentation

E. coli SCEcL3 and SC/NAR-05D04H were grown overnight at 37 °C in seed medium. The overnight cultures were diluted (1:9) into 48-well FlowerPlate® containing 1.8 mL fermentation medium (pH 6.8, adjusted by 25 % (w/v) ammonia) in BioLector (Beckman, USA). The fermentation was performed at 37 °C, 900 rpm for 48 h. The dissolved oxygen (DO), pH and temperature were monitored online, and DO was controlled at 40 %. The initial pH of the fermentation medium for all the strains was pH 6.8, and after the pH gradually decreased during fermentation, the parent strains were controlled at pH 6.8 or pH 6.0, while SC/NAR-05D04H strains were controlled at pH 6.0, using 5 % (w/

v) ammonia. After 48 h fermentation, samples were taken for measuring optical density, residual glucose and lysine titer. OD_{562} was measured by ultraviolet spectrophotometer and the titers of glucose and lysine were measured by SBA-40D biosensor analyzer (Shandong Academy of Science, Shandong Province, China).

3. Results

3.1. Effects of DsrA and Hfq expression levels on E. coli cell growth at low pH

To develop a tool for precise modulation of DsrA and Hfq expression, we utilized two promoters, P_{cymR} [34] and P_{tac} [37], which exhibited comparable strength (Fig. 1A). The fluorescence output of these promoters ranged from 0 to 16,000 a.u. upon addition of 0–200 μM cumate for P_{cymR} or 0–500 μM IPTG for P_{tac} (Fig. S2). DsrA and Hfq were then placed under the control of P_{cymR} and P_{tac}, respectively, and cloned into plasmid pACYC184. To minimize any potential impact on the structure and biological activity of the DsrA due to the introduction of unnecessary nucleotides at its 5′ end, we appended a ribozyme HH downstream of P_{cymR} [38]. This inducible DsrA-Hfq module was transferred into MG1655 strain, yielding strain MG/CDTH, for the growth assay upon pH 4.5. As shown in Fig. 1A, the increase of Hfq expression, in terms of IPTG addition from 0 to 500 μM, resulted in a significant increase in the final OD_{600} value from 0.318 ± 0.009 to 0.555 ± 0.006, but did not significantly alter the growth rate (Table S4). Changes in DsrA expression levels had no significant impact on the final OD_{600}, while a significant decrease in growth rate from 1.142 ± 0.002 to 0.897 ± 0.016 was observed when DsrA expression was induced at a high level by 200 μM cumate. We thought that this decrease was caused by the effect of high concentration of cumate on growth rather than the high-level expression of DsrA (Table S5) [34]. We then conducted another construct (MG/SDTH) using the P_{sal} promoter to express DsrA, which can transcribe an RNA with a native 5′ end and have a lower strength compared to P_{cymR} (Fig. S3). Similar results were observed with this new construct, and the overexpression of DsrA was no significant impact on cell growth as expected (Fig. S3, Table S6).

To gain further insights, we replaced the inducible promoters with five constitutive promoters, ranging from strong to weak, namely J23104, J23100, J23110, J23105, J23116 (Fig. S4). We constructed pCon series plasmids by using three strong promoters (more than 5000 a.u.) to control Hfq and two weak promoters (less than 2000 a.u.) to control DsrA (Fig. 1B). Thus, six strains were generated with different DsrA-Hfq expression cassettes. The growth assay at pH 4.5 showed that as the strength of promoter controlling Hfq increased, the final OD_{600} exhibited an upward trend from 0.572 ± 0.016 to 0.761 ± 0.022, which was consistent with the above results (Fig. 1B). Compared to wild-type *E. coli* MG1655, the final OD_{600} of MG/Con-05D00H, MG/Con-05D10H, MG/Con-16D00H and MG/Con-16D10H significantly increased by 79.9%, 65.6%, 74.9% and 62.7%, respectively (Table S7). However, the growth rate decreased from 0.966 ± 0.060 to 0.821 ± 0.160, when the expression levels of Hfq increased (Fig. 1B). For the strains MG/Con-05D04H and MG/Con-16D04H, the expression of Hfq with the strongest promoter J23104 severely inhibited growth rate of the cells in the early stage. These results contrast with those observed when using inducible promoters, where we speculate that the continuous accumulation of Hfq under constitutive promoters may have negatively impacted cell growth.

In addition, to demonstrate the auxiliary effect of DsrA, we constructed plasmids expressing Hfq solely as a control. It was worth noting that, without co-expression of DsrA, we only obtained the correct transformants when Hfq was expressed by promoter J23110 (the plasmid named pCon-10H), which is the weakest of these three promoters. This strain, MG/Con-10H, exhibited similar growth profile to strains MG/Con-05D04H and MG/Con-16D04H, with a growth rate of 0.413 ± 0.024. We were unable to obtain the correct constructions when

expressing Hfq using the other two more strong promoters (*i.e.* J23104 and J23100). All ten of the transformants for each construct exhibited single base mutations or single base deletions, leading to changes in the promoter sequences or premature termination of Hfq translation (data not shown).

These results indicated high expression levels of Hfq are toxic for the cells, as it had been shown to negatively affect the DNA repair [39] and cell division [40,41]. This could be attributed to the multifaceted regulatory effects of Hfq, which is capable of interacting with various RNA molecules. Although overexpression of DsrA did not significantly impact biomass and growth rate in *E. coli* MG1655, we can still believe that maintaining a relatively low level of DsrA expression can help to reduce the toxic effect of Hfq on cells. Excessive DsrA may compete with other RNA molecules for Hfq that establish an optimal homeostatic state [42–44]. Taken together, our results suggest that the Hfq expression should be strict regulated and combined with the over-expression of a sRNA like DsrA to engineer a synthetic tolerance strain.

3.2. Characterization of CymR-based negative auto-regulation circuit

We further construct a negative autoregulation (NAR) circuit to control the expression of DsrA-Hfq [31–34]. We opted the CymR-based NAR [34] due to its minimal impact on cell growth and the cost-effectiveness of the inducer cumate compared to the TetR-based NAR circuit [31,32]. Subsequently, the CymR regulator-based NAR circuits were characterized and compared to negative regulation (NR) switches using sfGFP as a reporter in different media (M9 vs. LBG), strains (DH10B vs. MG1655), and pHs (pH 7.0 vs. pH 4.5) (Fig. 2A). To evaluate the robustness of the circuits, we introduced the D value as a measure of deviation of the circuits output under virous conditions (see methods). Thus, we can calculate the fluorescence output ratio under different conditions and converted it to a logarithmic base 10 scale for comparison. A smaller D value indicates a smaller difference in expression level when the environment changes, suggesting a more robust circuit. Additionally, we hypothesize that if the D values converge to a certain value at different inducer concentrations, the circuit should be considered robust. While it is expected for environmental changes to affect circuit output, if these changes are consistent, their effects can be predicted and used to inform circuit design.

As shown in Fig. 2B, the deviation of the circuit output in various media (*i.e.* D_M) under pH 7.0 of NAR ranged from 0.31 to 0.63, which was more stable compared to NR that ranged from 0.00 to 0.97. At pH 4.5, the D_M of both circuits increased (0.34–1.32 for NAR and 0.35–1.80 for NR) compared to pH 7.0. In M9 medium, the deviation of the circuit output in virous strains (*i.e.* D_S) of NAR ranged from 0.17 to 0.79 at pH 7.0 and 0.02 to 0.26 at pH 4.5, while the D_S of NR ranged from 0.00 to 1.03 at pH 7.0 and 0.01 to 2.39 at pH 4.5. In MG1655, the effect of pH on the circuits was more significant in M9 medium compared to those in LBG medium. D_{pH} for NAR and NR ranged from 0.07 to 0.35, and 0.22 to 1.50, respectively, in LBG medium, ranged from 0.21 to 0.91, and 0.18 to 2.75, respectively, in M9 medium. Additionally, the coefficient of variation (CV) of D values in the NAR circuits was smaller than those for the NR switches (0.27–0.63 vs. 0.57–1.74), indicating that the outputs of the NAR circuits were more predictable when the environment changed, such as media, strains or pHs. We also found that the expression curves for NAR circuits were more linear than those for NR switch at different conditions with lower slopes (R^2 of 0.92–0.99 vs. 0.80–0.97, slope of 0.36–0.73 vs. 1.00–1.63, Fig. S5). These results suggested that the NAR circuit is less sensitive to variations in inducer concentration, which is important for fine-tuning the expression of acid-resistant module in an industrial setting.

At the single cell level, NAR circuits resulted in a more tightly clustered distribution of fluorescent output compared to the NR switches (Fig. S6). In both exponential and stationary phases, the outputs of NAR circuits and NR switches were similar, but distinct outcomes were observed for the constitutive expression constructs in these two growth
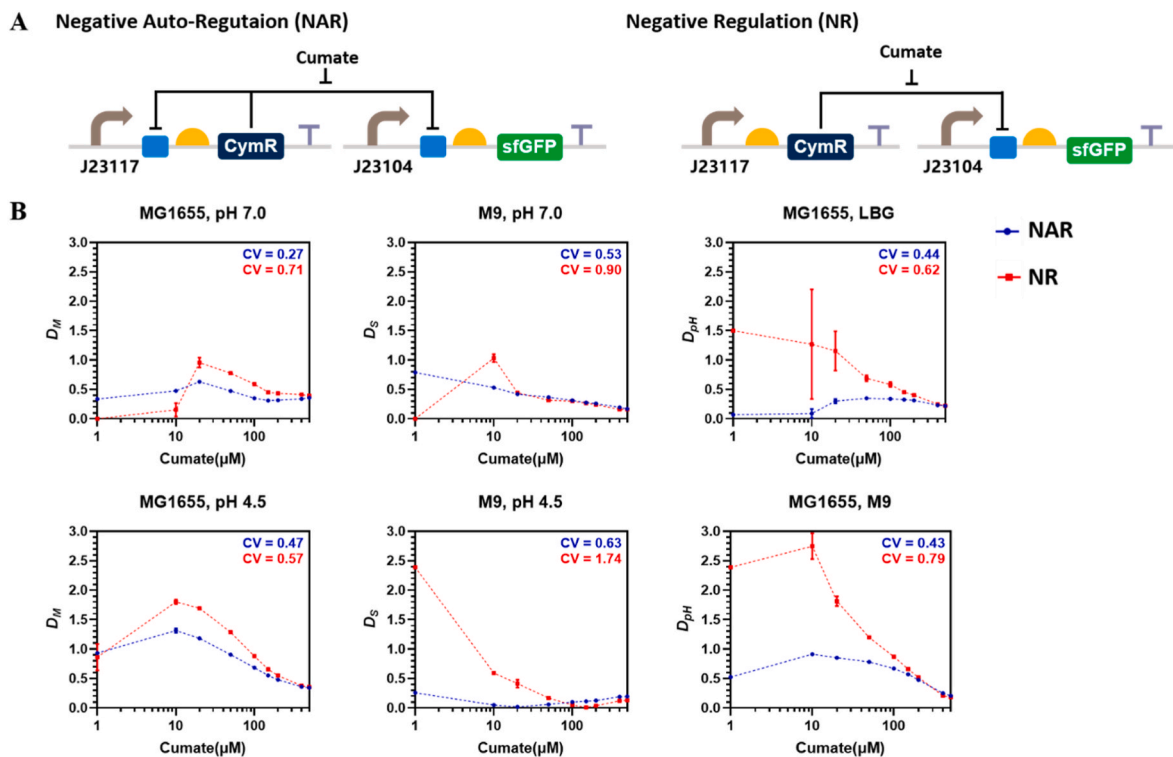
Fig. 2. NAR circuit performs better in robustness when encountering environment change. (A) Schematic representation of the reporter plasmid with NAR circuit (left) and NR switch (right). (B) The difference of output level in NAR circuit and NR switch when medium (two graphs on left), strain (two graphs in the middle) or pH (two graphs on right) change. The coefficients of variation of D values are at the upper right of each graph.

phases (Fig. S6C). These results suggested that the NAR circuits maintain a relatively consistent output at the single-cell level and is not influenced by cell growth stage [31,32], which may align with our objective of transferring the tolerance phenotype from lab strains and conditions to industrial strains and conditions.

3.3. Evaluation of the performance of auto-negative regulatory acid-resistant circuit on cell growth and productivity of an industrial lysine-producing strain

After understanding the characteristics of the DsrA-Hfq module and NAR circuit, we constructed six NAR acid-resistant circuits using different strength promoters to regulate the expression of DsrA and Hfq (Fig. 3A). In the lab strain MG1655, final OD_{600} for the strains harboring the NAR acid-resistant circuit after cultivating for 24 h in LBG (pH 4.5) ranged from 0.335 ± 0.003 to 0.425 ± 0.006, compared to the wild type MG1655 (0.353 ± 0.008). Among these six constructs, strain MG/NAR-05D04H with 100 μM cumate exhibited the highest biomass increase of 20.4% compared to wild type strain (Fig. 3C and Table S8). To demonstrate the benefit of NAR, we also construct a NR switch-controlled DsrA-Hfq construct, NR-05D04H (Fig. 3B). However, only 8.2 % increase in biomass was obtained for MG/NR-05D04H with the addition of 20 μM cumate, and further increases in cumate concentration did not yield any additional improvement. Moreover, higher level of DsrA-Hfq expression generally resulted in greater enhancement of biomass with only a slight impact on growth rate (Fig. 3D and Table S8). These results indicate that NAR circuit is effective in achieving the need for precise control of the DsrA-Hfq module expression.

We then transferred the NAR circuit-controlled DsrA-Hfq module pNAR-05D04H, and the controls including four constitutive promoter-controlled DsrA-Hfq modules, which were pCon-05D00H, pCon-05D10H, pCon-16D00H, and pCon-16D10H, and a NR switch-controlled DsrA-Hfq module pNR-0504H into the industrial lysine-producing strain *E. coli* SCEcL3, respectively. Fermentations were conducted in industrial

medium at a starting pH of 6.8 and without pH control, which will decrease to around 5 after 48 h cultivation (see methods). The constitutive promoter-controlled DsrA-Hfq modules severely impaired the growth of *E. coli* SCEcL3, making them unsuitable for fermentation, although they were able to increase biomass of a lab strain MG1655 by over 62.7 % (Fig. S7). For the NAR or NR controlled DsrA-Hfq module, we selected the best condition, which involved adding 100 μM cumate to induce sufficient expression of DsrA and Hfq (Fig. 3C). As shown in Fig. 4A and B, when cumate added at the beginning of the fermentation (*i.e.* 0 h), the OD_{562} values for strains SC/NAR-05D04H and SC/NR-05D04H were 5.69 ± 0.55 and 5.68 ± 0.02, respectively, representing a decrease of 5.2 % and 5.4 % compared to the parental strains. Lysine titers increased by 50 % and 75 %, respectively, reaching 3.00 ± 0.05 g/L and 3.50 ± 0.05 g/L (Table S9). When inducer was added at 3 h, the OD_{562} values for the strains SC/NAR-05D04H and SC/NR-05D04H increased by 19.9 % and 14.5 % compared to the parental strains, respectively, reaching 7.20 ± 0.04 and 6.88 ± 0.42. Lysine titers increased by 250 % and 150 %, respectively, reaching 7.00 ± 0.05 g/L and 5.00 ± 0.05 g/L.

In terms of addition time of cumate, inducing at 3 h resulted in higher biomass and lysine production compared to those inducing at 0 h. In terms of acid-resistant construct, SC/NAR-05D04H exhibit the best performance when the inducer was added at 3 h. It was also observed that the higher OD_{562} values corresponded to higher lysine titer and glucose consumption, as well as slower decrease in pH (Fig. S8). Taken together, the NAR circuit robustiously controls the gene expression mode, allowing for the transfer of acid-tolerant phenotype of the DsrA-Hfq module observed in laboratory strains to the industrial strains.

We then further evaluated the SC/NAR-05D04H strain in 2-mL FlowerPlate® on the BioLector microreactor, allowing for the simultaneous testing of 48 samples and control of pH levels at 6.8 or 6.0 through the addition of 5 % (w/v) ammonia solution. Under pH 6.0, the engineered strain SC/NAR-05D04H achieved a final OD_{562} of 3.02 ± 0.02 and a lysine titer of 2.95 ± 0.07 g/L when 50 μM cumate was added,
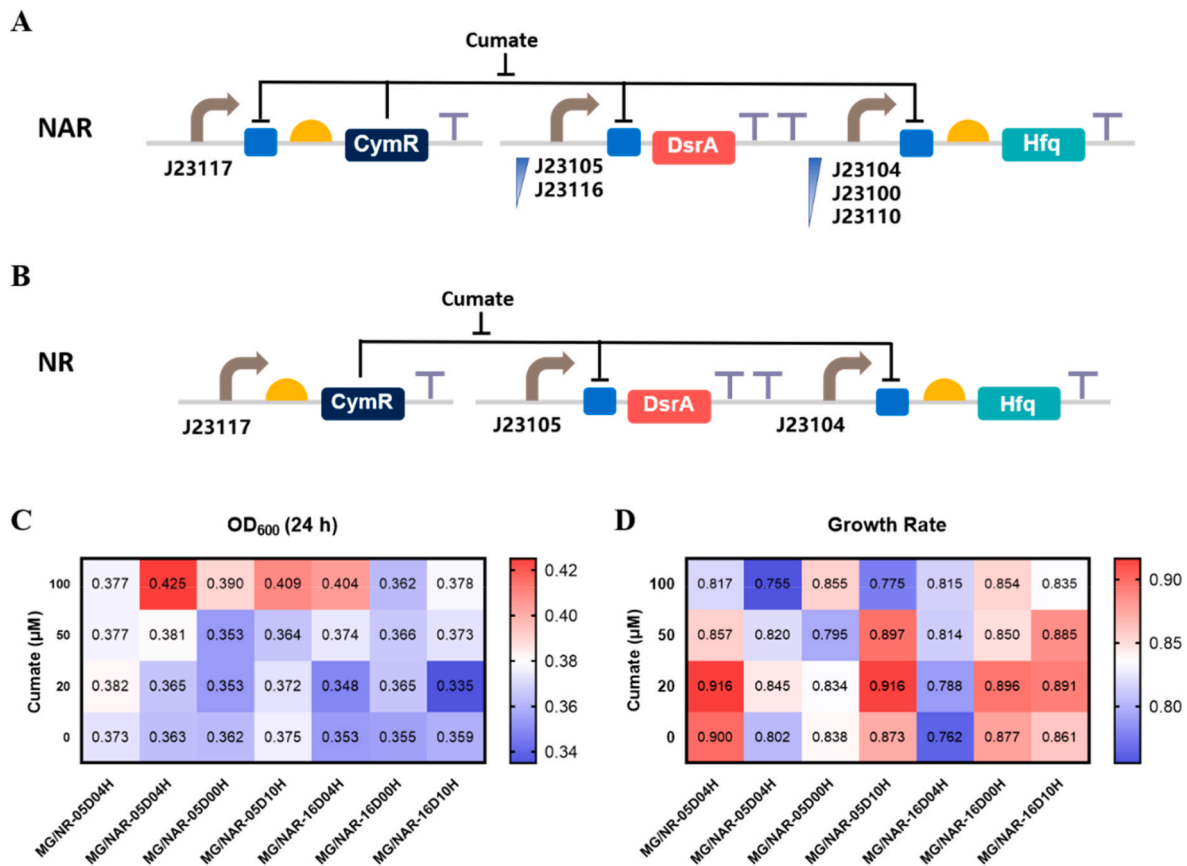
Fig. 3. NAR-05D04H increased biomass of *E. coli* MG1655 among all other acid-resistant circuits. (A) Schematic representation of the pNAR series plasmids. (B) Schematic representation of plasmid pNR-05D04H with negative regulatory acid-resistant circuit. (C) Final OD_{600} of the strains harbored pNAR series or pNR-05D04H plasmid in LBG medium (pH 4.5). (D) Growth rate of the strains harbored pNAR series or pNR-05D04H plasmid in LBG medium (pH 4.5).
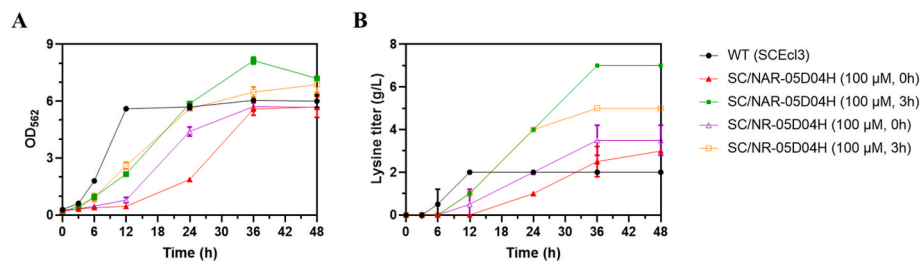

Fig. 4. Auto-negative regulatory acid-resistant circuit increased the biomass and thus its lysine titer of industrial lysine-producing strain. Plots of cell growth in terms of OD_{600} (A), and lysine titer (B).

compared to 2.24 ± 0.01 and 2.6 ± 0.10 g/L without cumate addition (Fig. S9). This represents a 2.73 % and 7.27 % increase in OD_{562} and lysine production, respectively, compared to the parental strain SCEcL3 at pH 6.8 (2.94 ± 0.21 and 2.75 ± 0.07 g/L), and a 202 % and 195 % increase compared to the parental strain at pH 6.0 (1.48 ± 0.01 and 1.95 ± 0.07 g/L). These results indicate that under moderate acid stress (pH 6.0), SC/NAR-05D04H shows significant enhancements in cell growth and lysine production, performing similarly to the parental strain under near-neutral conditions (pH 6.8).

4. Discussion

Microorganism breeding with a tolerance phenotype is a crucial strategy for green biomanufacturing as it helps conserving energy and reducing emissions [21,45–47]. In this study, we demonstrated effectiveness of the CymR-based NAR circuit in strictly and robustly

controlling the expression of the DsrA-Hfq module. This circuit enabled us to transfer the optimized acid-tolerance phenotype from the lab strain *E. coli* MG1655 to the industrial lysine-producing strain *E. coli* SCEcL3. In the fermentation without pH control, the best circuit NAR-05D04H, which involved the addition of an inducer at 3 h, achieved a remarkable 250 % increase in lysine titer compared to the parent strain. Additionally, this circuit enabled the strain to achieve a 7.27 % increase in lysine titer at pH 6.0 compared to the parent strain at pH 6.8. In our previous work, we employed a stepwise manner to screen nearly a thousand clones to obtain a four-gene module involved in proton consumption periplasmic chaperone, and reactive oxygen species (ROS) scavengers to improve the lysine productivity of the industrial stain [36]. The best strain showed a significant 16 %–18 % increase in lysine yield at pH 6.0 compared to the parent strain at pH 6.8.

Gene circuits are often studied under highly controlled conditions that differ greatly from real-world applications to minimize the

influence of complex factors [45,46]. This presents a major challenge in transitioning from bench experiments to pilot plant scale. Our study showed a practical application of a synthetic gene circuit that can effectively elicit a desired phenotype in both laboratory and industrial strains and conditions. Fluctuations in the production rate of transcriptional regulators can arise from variations in the cell's metabolic capacity and regulatory network [47,48]. The CymR-based NAR circuit somehow could accommodate these fluctuations, ensuring consistent performance across different conditions such as media, strains, and pH levels. We have also suggested that CV of the *D* value could serves as an efficient measure of circuit performance in these varying conditions. Furthermore, NAR circuit has the capability to be coupled with other circuits, enhancing its robustness in fermentation systems. For instance, it can be coupled with a metabolite addiction circuit to improve overall performance [49]. Coupling it with linear weak positive feedback circuits allows the construction of a synthetic robust perfect adaptation system, which exhibits a pulse-like gene expression profile and enables precise expression of a specific amount of protein at a specific time [50].

Our study revealed that the overexpression of Hfq, rather than DsrA, may be the key factor in enhancing the acid-tolerance of cells within the DsrA-Hfq module [27]. Hundreds of sRNA have been identified in *E. coli*, and appropriately one-third of these sRNAs bind to the homo-hexameric Hfq protein on its proximal, rim or distal face, and compete with each other for binding sites [24,44,51]. Class II sRNA, *e.g.* ChiX and MgrR, generally have a stronger binding affinity to Hfq than Class I sRNA, *e.g.* DsrA. In addition, DsrA can coexist with other Hfq-dependent sRNA on Hfq, but their sRNA function were suggested to be reduced [44]. The weaker binding affinity of DsrA to Hfq may explain why it unable to enhance the acid tolerant of *E. coli* at moderate low pH (pH 4.5) simply by increasing its expression level without co-overexpression of Hfq. Additionally, DsrA could effectively reduce the cytotoxicity caused by high levels of Hfq overexpression, likely because excessive DsrA completely binds to Hfq. Our study highlighted the interaction between DsrA and Hfq. Further engineering of DsrA-Hfq module could involve fusing Hfq binding sites from Class II sRNAs to DsrA, as well as introducing mutations to modulate binding affinity of Hfq to DsrA and other sRNAs, in order to further improve the acid resistance of this module [42,52].

Data availability

The datasets used in this study can be found in the Supplementary Material or requested to the corresponding author.

CRediT authorship contribution statement

Xiaofeng Yang: Investigation, Conceptualization, Supervision, Writing – review & editing. **Jingduan Yang:** Investigation, Methodology, Data curation, Writing – original draft. **Haozheng Huang:** Data curation. **Xiaofang Yan:** Writing – review & editing. **Xiaofan Li:** Writing – review & editing. **Zhanglin Lin:** Conceptualization, Funding acquisition, Supervision, Writing – review & editing.

Declaration of competing interest

The authors declare that they have no known competing financial interests or personal relationships that could have appeared to influence the work reported in this paper.

Acknowledgments

Appendix A. Supplementary data

References

[1] Zaldivar J, Martinez A, Ingram LO. Effect of alcohol compounds found in hemicellulose hydrolysate on the growth and fermentation of ethanologenic Escherichia coli. Biotechnol Bioeng 2000;68(5):524–30. https://doi.org/10.1002/(Sici)1097-0290(20000605)68:5<524::Aid-Bit6>3.3.Co;2-K.

[2] Abdel-Banat BM, Hoshida H, Ano A, Nonklang S, Akada R. High-temperature fermentation: how can processes for ethanol production at high temperatures become superior to the traditional process using mesophilic yeast? Appl Microbiol Biotechnol 2010;85(4):861–7. https://doi.org/10.1007/s00253-009-2248-5.

[3] Doi H, Hoshino Y, Nakase K, Usuda Y. Reduction of hydrogen peroxide stress derived from fatty acid beta-oxidation improves fatty acid utilization in Escherichia coli. Appl Microbiol Biotechnol 2014;98(2):629–39. https://doi.org/10.1007/s00253-013-5327-6.

[4] Xu K, Lee YS, Li J, Li C. Resistance mechanisms and reprogramming of microorganisms for efficient biorefinery under multiple environmental stresses. Synth Syst Biotechnol 2019;4(2):92–8. https://doi.org/10.1016/j.synbio.2019.02.003.

[5] Trcek J, Mira NP, Jarboe LR. Adaptation and tolerance of bacteria against acetic acid. Appl Microbiol Biotechnol 2015;99(15):6215–29. https://doi.org/10.1007/s00253-015-6762-3.

[6] Ko Y, Seol E, Sekar BS, Kwon S, Lee J, Park S. Metabolic engineering of klebsiella pneumoniae J2b for co-production of 3-hydroxypropionic acid and 1,3-propanediol from glycerol: reduction of acetate and other by-products. Bioresour Technol 2017;244(1):1096–103. https://doi.org/10.1016/j.biortech.2017.08.099.

[7] Liu Y, Tang H, Lin Z, Xu P. Mechanisms of acid tolerance in bacteria and prospects in biotechnology and bioremediation. Biotechnol Adv 2015;33(7):1484–92. https://doi.org/10.1016/j.biotechadv.2015.06.001.

[8] Russell JB, DiezGonzalez F. The effects of fermentation acids on bacterial growth. Adv Microbiol 1998;39:205–34. https://doi.org/10.1016/S0065-2911(08)60017-X.

[9] Ahn JH, Seo H, Park W, Seok J, Lee JA, Kim WJ, et al. Enhanced succinic acid production by mannheimia employing optimal malate dehydrogenase. Nat Commun 2020;1970(1):11. https://doi.org/10.1038/s41467-020-15839-z.

[10] Hashimoto SI. Discovery and history of amino acid fermentation. Adv Biochem Eng Biotechnol 2017;159:15–34. https://doi.org/10.1007/10_2016_24.

[11] Guan N, Liu L. Microbial response to acid stress: mechanisms and applications. Appl Microbiol Biotechnol 2020;104(1):51–65. https://doi.org/10.1007/s00253-019-10226-1.

[12] Iyer MS, Pal A, Srinivasan S, Somvanshi PR, Venkatesh KV. Global transcriptional regulators fine-tune the translational and metabolic efficiency for optimal growth of Escherichia coli. mSystems 2021;6(2). https://doi.org/10.1128/mSystems.00001-21.

[13] Lin Z, Zhang Y, Wang J. Engineering of transcriptional regulators enhances microbial stress tolerance. Biotechnol Adv 2013;31(6):986–91. https://doi.org/10.1016/j.biotechadv.2013.02.010.

[14] Dragosits M, Mozhayskiy V, Quinones-Soto S, Park J, Tagkopoulos I. Evolutionary potential, cross-stress behavior and the genetic basis of acquired stress resistance in Escherichia coli. Mol Syst Biol 2013;643:9. https://doi.org/10.1038/msb.2012.76.

[15] Creamer KE, Ditmars FS, Basting PJ, Kunka KS, Hamdallah IN, Bush SP, et al. Benzoate- and salicylate-tolerant strains of Escherichia coli K-12 lose antibiotic resistance during laboratory evolution. Appl Environ Microbiol 2017;83(2). https://doi.org/10.1128/AEM.02736-16.

[16] Harden MM, He A, Creamer K, Clark MW, Hamdallah I, Martinez KA, et al. Acid-adapted strains of Escherichia coli K-12 obtained by experimental evolution. Appl Environ Microbiol 2015;81(6):1932–41. https://doi.org/10.1128/Aem.03494-14.

[17] Liu R, Liang L, Choudhury A, Bassalo MC, Garst AD, Tarasava K, et al. Iterative genome editing of Escherichia coli for 3-hydroxypropionic acid production. Metab Eng 2018;47:303–13. https://doi.org/10.1016/j.ymben.2018.04.007.

[18] Alper H, Moxley J, Nevoigt E, Fink GR, Stephanopoulos G. Engineering yeast transcription machinery for improved ethanol tolerance and production. Science 2006;314(5805):1565–8. https://doi.org/10.1126/science.1131969.

[19] Basak S, Geng HF, Jiang RR. Rewiring global regulator camp receptor protein (crp) to improve E. coli tolerance towards low pH. J Biotechnol 2014;173(1):68–75. https://doi.org/10.1016/j.jbiotec.2014.01.015.

[20] Gao X, Jiang L, Zhu L, Xu Q, Xu X, Huang H. Tailoring of global transcription sigma d factor by random mutagenesis to improve Escherichia coli tolerance towards low-pHs. J Biotechnol 2016;224:55–63. https://doi.org/10.1016/j.jbiotec.2016.03.012.

[21] Aquino P, Honda B, Jaini S, Lyubetskaya A, Hosur K, Chiu JG, et al. Coordinated regulation of acid resistance in Escherichia coli. BMC Syst Biol 2017;1(1):11. https://doi.org/10.1186/s12918-016-0376-y.

[22] Battesti A, Majdalani N, Gottesman S. The RpoS-mediated general stress response in Escherichia coli. Annu Rev Microbiol 2011;65:189–213. https://doi.org/10.1146/annurev-micro-090110-102946.

[23] Gaida SM, Al-Hinai MA, Indurthi DC, Nicolaou SA, Papoutsakis ET. Synthetic tolerance: three noncoding small RNAs, DsrA, ArcZ and RprA, acting supra-additively against acid stress. Nucleic Acids Res 2013;41(18):8726–37. https://doi.org/10.1093/nar/gkt651.

[24] Soper TJ, Doxzen K, Woodson SA. Major role for mRNA binding and restructuring in sRNA recruitment by Hfq. RNA 2011;17(8):1544–50. https://doi.org/10.1261/rna.2767211.

[25] Rodgers ML, O'Brien B, Woodson SA. Small RNAs and Hfq capture unfolded RNA target sites during transcription. Mol Cell 2023;83(9):1489–501. https://doi.org/10.1016/j.molcel.2023.04.003.

[26] Sedlyarova N, Shamovsky I, Bharati BK, Epshtein V, Chen JD, Gottesman S, et al. sRNA-mediated control of transcription termination in E. coli. Cell 2016;167(1):111–21. https://doi.org/10.1016/j.cell.2016.09.004.

[27] Lin Z, Li J, Yan X, Yang J, Li X, Chen P, et al. Engineering of the small noncoding RNA (sRNA) DsrA together with the sRNA chaperone Hfq enhances the acid tolerance of *Escherichia coli*. Appl Environ Microbiol 2021;87(10):e02923. https://doi.org/10.1128/AEM.02923-20. 20.

[28] Gottesman S. Trouble is coming: signaling pathways that regulate general stress responses in bacteria. J Biol Chem 2019;294(31):11685–700. https://doi.org/10.1074/jbc.REV119.005593.

[29] Brophy JA, Voigt CA. Principles of genetic circuit design. Nat Methods 2014;11(5):508–20. https://doi.org/10.1038/nmeth.2926.

[30] Bradley RW, Buck M, Wang B. Tools and principles for microbial gene circuit engineering. J Mol Biol 2016;428(5 Pt B):862–88. https://doi.org/10.1016/j.jmb.2015.10.004.

[31] Dublanche Y, Michalodimitrakis K, Kummerer N, Foglierini M, Serrano L. Noise in transcription negative feedback loops: simulation and experimental analysis. Mol Syst Biol 2006;41:2. https://doi.org/10.1038/msb4100081.

[32] Klumpp S, Zhang Z, Hwa T. Growth rate-dependent global effects on gene expression in bacteria. Cell 2009;139(7):1366–75. https://doi.org/10.1016/j.cell.2009.12.001.

[33] Nevozhay D, Adams RM, Murphy KF, Josic K, Balazsi G. Negative autoregulation linearizes the dose-response and suppresses the heterogeneity of gene expression. Proc Natl Acad Sci USA 2009;106(13):5123–8. https://doi.org/10.1073/pnas.0809901106.

[34] Guan Y, Chen X, Shao B, Ji X, Xiang Y, Jiang G, et al. Mitigating host burden of genetic circuits by engineering autonegatively regulated parts and improving functional prediction. ACS Synth Biol 2022;11(7):2361–71. https://doi.org/10.1021/acssynbio.2c00073.

[35] Gibson DG, Young L, Chuang R-Y, Venter JC, Hutchison III CA, Smith HO. Enzymatic assembly of DNA molecules up to several hundred kilobases. Nat Methods 2009;6(5):343. https://doi.org/10.1038/nmeth.1318. U41.

[36] Yao X, Liu P, Chen B, Wang X, Tao F, Lin Z, et al. Synthetic acid stress-tolerance modules improve growth robustness and lysine productivity of industrial *Escherichia coli* in fermentation at low pH. Microb Cell Factories 2022;68(1):21. https://doi.org/10.1186/s12934-022-01795-4.

[37] Meyer AJ, Segall-Shapiro TH, Glassey E, Zhang J, Voigt CA. *Escherichia coli* "marionette" strains with 12 highly optimized small-molecule sensors. Nat Chem Biol 2019;15(2):196–204. https://doi.org/10.1038/s41589-018-0168-3.

[38] Gao Y, Zhao Y. Self-processing of ribozyme-flanked RNAs into guide RNAs in vitro and in vivo for CRISPR-mediated genome editing. J Integr Plant Biol 2014;56(4):343–9. https://doi.org/10.1111/jipb.12152.

[39] Chen J, Gottesman S. Hfq links translation repression to stress-induced mutagenesis in *E. coli*. Genes Dev 2017;31(13):1382–95. https://doi.org/10.1101/gad.302547.117.

[40] Gruetzner J, Remes B, Eisenhardt KMH, Scheller D, Kretz J, Madhugiri R, et al. sRNA-mediated RNA processing regulates bacterial cell division. Nucleic Acids Res 2021;49(12):7035–52. https://doi.org/10.1093/nar/gkab491.

[41] Zambrano N, Guichard PP, Bi Y, Cayrol B, Marco S, Arluison V. Involvement of HFq protein in the post-transcriptional regulation of *E. coli* bacterial cytoskeleton and cell division proteins. Cell Cycle 2009;8(15):2470–2. https://doi.org/10.4161/cc.8.15.9090.

[42] Park S, Prévost K, Heideman EM, Carrier M-C, Azam MS, Reyer MA, et al. Dynamic interactions between the RNA chaperone Hfq, small regulatory RNAs, and mRNAs in live bacterial cells. Elife 2021;10:e64207. https://doi.org/10.7554/eLife.64207.

[43] Vogel J, Luisi BF. Hfq and its constellation of RNA. Nat Rev Microbiol 2011;9(8):578–89. https://doi.org/10.1038/nrmicro2615.

[44] Roca J, Santiago-Frangos A, Woodson SA. Diversity of bacterial small RNAs drives competitive strategies for a mutual chaperone. Nat Commun 2022;2449(1):13. https://doi.org/10.1038/s41467-022-30211-z.

[45] Bashor CJ, Patel N, Choubey S, Beyzavi A, Kondev J, Collins JJ, et al. Complex signal processing in synthetic gene circuits using cooperative regulatory assemblies. Science 2019;364(6440):593–7. https://doi.org/10.1126/science.aau8287.

[46] Bradley RW, Buck M, Wang B. Tools and principles for microbial gene circuit engineering. J Mol Biol 2016;428(5):862–88. https://doi.org/10.1016/j.jmb.2015.10.004.

[47] Elowitz MB, Levine AJ, Siggia ED, Swain PS. Stochastic gene expression in a single cell. Science 2002;297(5584):1183–6. https://doi.org/10.1126/science.1070919.

[48] Kaern M, Elston TC, Blake WJ, Collins JJ. Stochasticity in gene expression: from theories to phenotypes. Nat Rev Genet 2005;6(6):451–64. https://doi.org/10.1038/nrg1615.

[49] Lv Y, Gu Y, Xu J, Zhou J, Xu P. Coupling metabolic addiction with negative autoregulation to improve strain stability and pathway yield. Metab Eng 2020;61:79–88. https://doi.org/10.1016/j.ymben.2020.05.005.

[50] Sun Z, Wei W, Zhang M, Shi W, Zong Y, Chen Y, et al. Synthetic robust perfect adaptation achieved by negative feedback coupling with linear weak positive feedback. Nucleic Acids Res 2022;50(4):2377–86. https://doi.org/10.1093/nar/gkac066.

[51] Bak G, Lee J, Suk S, Kim D, Young Lee J, Kim K-s, et al. Identification of novel sRNAs involved in biofilm formation, motility and fimbriae formation in *Escherichia coli*. Sci Rep 2015;15287(1):5. https://doi.org/10.1038/srep15287.

[52] Bao SH, Jiang H, Zhu LY, Yao G, Han PG, Wan XK, et al. A dynamic and multilocus metabolic regulation strategy using quorum-sensing-controlled bacterial small RNA. Cell Rep 2021;109413(3):36. https://doi.org/10.1016/j.celrep.2021.109413.